Journal of Molecular Liquids 319 (2020) 114157

Contents lists available at ScienceDirect

Journal of Molecular Liquids

journal homepage: www.elsevier.com/locate/molliq

Electronic and nonlinear optical properties of 2-(((5-aminonaphthalen-1-yl)imino)methyl)phenol: Experimental and time-dependent density functional studies

Nathanael Damilare Ojo [a,*], Rui Werner Krause [b], Nelson Okpako Obi-Egbedi [a]

[a] Department of Chemistry, Faculty of Science, University of Ibadan, Ibadan, Nigeria
[b] Department of Chemistry, Faculty of Science, Rhodes University, P.O. Box 94, Grahamstown 6140, Eastern Cape, South Africa

ARTICLE INFO

Article history:
Received 2 May 2020
Received in revised form 17 August 2020
Accepted 26 August 2020
Available online 29 August 2020

Keywords:
Nonlinear optical property
Solvatochromism
Fluorescence
Schiff base
Time-dependent density functional theory

ABSTRACT

In this study, solvent dependence of electronic and nonlinear optical properties of a new Schiff base, 2-(((5-aminonaphthalen-1-yl)imino)methyl) phenol (DANNAB), has been investigated. Electronic and optical properties of the Schiff base studied using Uv-visible absorption and fluorescence spectroscopic techniques in solution show that the Schiff base exhibits fluorescence with a quantum yield of 0.21 and a Stokes shift of 39 nm. Quantum chemical calculations were performed on the Schiff base at time-dependent density functional level of theory using Becke-3-Lee-Yang-Parr method with 6-311++G(d,p) basis set. Solvent dependence of the excited state energies (EE), energy gap (ΔE), first-order (β) and second-order (γ) hyperpolarizabilities were studied in gas, cyclohexane and ethanol. The medium perturbed the energy levels which implies that the reactivity, activity and stability of the system are solvent sensitive. The γ is more than thirty times higher than urea (standard NLO material) and this property is further enhanced in less polar medium. Small ΔE and large hyperpolarizabilities obtained for this system suggest its good potential in photonics and nonlinear optical devices.

1. Introduction

Organic systems with π-electrons and heteroatoms possess properties for optoelectronic applications as optical devices and organic semiconductors [1]. However, their efficiencies for photoluminescent and nonlinear optical (NLO) applications can either be enhanced or quenched based on the perturbing effect of the solvating medium [2–3]. A Schiff base is one of such organic systems with an extra merit of easy synthetic route.

Based on the research work of Hugo Schiff on aniline and its derivatives, the German chemist discovered the reaction routes to synthesizing organic systems with imine (C=N) functional group. These imine systems were later named after the pioneer researcher as Schiff base [4–5]. Due to the presence of imine group, the organic compounds were found to possess biological, electronic and optical properties [6–12]. These vast potentials motivate relentless effort in modelling, designing and synthesizing Schiff bases for a wide range of applications such as novel drug designs and delivery, optoelectronics, materials and corrosion science [8–16]. Due to their ease of tuneability, Schiff bases are versatile organic systems and have been adapted for not only biological applications but also for industrial purposes. They have been reported to possess chemosensing, chelating, photochromic, thermochromic, nonlinear optical limiting and fluorescent properties [17–21]. These potentials could majorly be attributed to the presence of azomethine (C=N) functional group in the system.

Schiff bases of benzaldehyde have been reported to possess excellent antimalarial, antibacterial, antifungal, anthelminthic and anticancer potentials and they have, consequently, been explored in drug design and delivery [22–25]. Also, recent researches on imine compounds have shown that electron richness of amines coupled with rigidity of the fused aromatic rings confers on them excellent photophysical properties [26–28]. While considering ease of synthesis and cost of production, naphthalene-based Schiff bases have been found to present good electronic, optical and biological properties which could be explored in novel drug synthesis, organic light-emitting diodes and nonlinear optical devices [29–33]. In spite of these vast potentials of fused aromatic Schiff bases, their effective use for photoluminescent applications such as luminescent solar concentrator has been limited due to small Stokes shift (Δλ = 5–20 nm) which results into significant spectral overlap and photon reabsorption problem [34].

Recent advances in quantum chemical calculations of electronic and optical properties of organic systems have shown time-dependent density functional theory (TD-DFT) to be accurate and computationally less

* Corresponding author.
E-mail address: dammynath@yahoo.com (N.D. Ojo).

https://doi.org/10.1016/j.molliq.2020.114157
0167-7322/

costly in predicting excited state properties of small to large molecules [35–36]. When coupled with hybrid exchange and correlation method like Becke-3-Lee-Yang-Parr (B3LYP), TD-DFT reproduces experimental excited state energies, polarizabilities and hyperpolarizabilities especially when combined with split valence basis sets with diffuse and polarization functions such as 6–311++G(d,p) [37–40]. The choice of 6–311++G(d,p) basis set with polarization and diffuse functions on hydrogen and non-hydrogen atoms accounts for the polarization of electron density of atoms in applied electric field and the intra-(inter-)molecular interactions essential in calculating dipole moment, (hyper)polarizabilities and excited state properties [41–45]. However, these electronic and nonlinear optical properties have been reported to be solvent sensitive, that is, the applicability of the system can be enhanced or damped based on solute-solvent interaction [40,46–47].

Therefore, the aim of this research is to investigate the nonlinear optical and electronic properties of 2-(((5-aminonaphthalen-1-yl)imino) methyl)phenol in different solvent system.

2. Calculation

All calculations were conducted on Gaussian '09 programme [48]. The geometry of the Schiff base was fully optimized and the vibrational modes of the optimized structure calculated at time-dependent-density functional level of theory using B3LYP/6-311++G(d,p) method with diffuse functions and polarization functions on hydrogen and non-hydrogen atoms [49]. Excited state energies (EE) were then computed in gas, cyclohexane and ethanol. The solvent was modelled as a continuum of dielectric using polarizable continuum model [2,49–50]. Quantum chemical parameters describing the polarity, linear optical and nonlinear properties of the system such as dipole moment (μ), polarizability (α), first order hyperpolarizability (β_{tot}) and second-order hyperpolarizability (γ) were computed from their multipolar components. The static dipole moment (μ) was computed from its x, y and z components using Eq. (1)

$$\mu = \left(\mu_x^2 + \mu_y^2 + \mu_z^2\right)^{\frac{1}{2}} \tag{1}$$

The polarizability, α, was calculated from the diagonal matrices of its quadrupolar components as shown from Eq. (2) and the anisotropy of polarizability calculated using Eq. (3) from diagonal and off-diagonal components.

$$\alpha = {}^{1}/_{3}\left(\alpha_{xx} + \alpha_{yy} + \alpha_{zz}\right) \tag{2}$$

$$\Delta\alpha = \frac{1}{\sqrt{2}}\left[\left(\left(\alpha_{xx}-\alpha_{yy}\right)^2 + \left(\alpha_{yy}-\alpha_{zz}\right)^2 + \left(\alpha_{zz}-\alpha_{xx}\right)^2\right) + 6\alpha_{xy}^2 + 6\alpha_{xz}^2 + 6\alpha_{yz}^2\right]^{1/2} \tag{3}$$

The 27 components of 3D matrix of first order hyperpolarizability were reduced by Kleimann symmetry into a 10-component matrix [51]. The β components reported in Gaussian '09 output files were further processed using Eqs. (4)–(7) to obtain the total first order hyperpolarizability (β_{tot}), which was converted to S.I. unit using Eq. (9). The second-order hyperpolarizability (γ) was calculated from the hexadecapolar components (Eq. (8)) and converted to S.I. unit using Eq. (10) [42]. The first-order and second-order hyperpolarizabilities are related to the second harmonic generation (SHG) and third harmonic generation (THG) applications of an NLO material, respectively, and can be compared with the hyperpolarizabilities of urea which is a standard nonlinear optical material.

$$\beta_{tot} = \left(\beta_x^2 + \beta_y^2 + \beta_z^2\right)^{1/2} \tag{4}$$

β_x, β_y and β_z were computed using:

$$\beta_x = \beta_{xxx} + \beta_{xyy} + \beta_{xzz} \tag{5}$$

$$\beta_y = \beta_{xxy} + \beta_{yyy} + \beta_{yzz} \tag{6}$$

$$\beta_z = \beta_{xxz} + \beta_{yyz} + \beta_{zzz} \tag{7}$$

$$\gamma = \frac{1}{5}\left(\gamma_{xxxx} + \gamma_{yyyy} + \gamma_{zzzz} + 2\gamma_{xxyy} + 2\gamma_{xxzz} + 2\gamma_{yyzz}\right) \tag{8}$$

$$1\ \text{a.u.} = 3.206361 \times 10^{-53}\ \text{C}^3\text{m}^3\text{J}^{-2}\ (\text{for}\ \beta_{tot}) \tag{9}$$

$$1\ \text{a.u.} = 6.235377 \times 10^{-65}\ \text{C}^4\text{m}^4\text{J}^{-3}\ (\text{for}\ \gamma) \tag{10}$$

Also, quantum chemical descriptors for the chemical reactivity, stability and selectivity such as energy gap (ΔE), energies of the Highest Occupied Molecular Orbital (E_{HOMO}) and Lowest Unoccupied Molecular Orbital (E_{LUMO}) were calculated and reported.

3. Experimental

3.1. General experimental

All reagents were of commercial grade and used without further purification. Ethanol was doubly distilled according to standard procedure. 1,5-diaminonaphthalene and 2-hydroxybenzaldehyde were purchased from Aldrich and used without further purification.

^{1}H, ^{13}C, ^{13}C– DEPT 135, HSQC and ^{1}H—^{1}H COSY spectra of the sample were obtained on a Bruker Ultrashield-300 NMR spectrometer in deuterated chloroform ($CDCl_3$) using tetramethylsilane (TMS) as internal standard. Attenuated Total Reflectance Fourier Transform Infrared (ATR-FTIR) spectrum of the synthesized sample was recorded in the solid state on a Perkin Elmer (Spectrum 100) ATR-FTIR spectrophotometer mounted with Diamond-ZnSe crystal from 4000 to 650 cm^{-1}. The mass spectra were obtained on Bruker Compact high-resolution Electrospray Ionization Quadrupole Time-of-Flight (HR-ESI-Q-TOF MS/MS) mass spectrometer. The uncorrected melting point was determined on a Gallenkamp instrument. The Uv-vis absorption spectrum was recorded on a Perkin Elmer Lambda 25 double beam Uv-vis spectrophotometer in ethanol at ambient temperature using a quartz cuvette of 1 cm path length in the concentration range of 10^{-5} M. Emission spectrum of the compound was obtained on a Varian Cary Eclipse Fluorescence Spectrophotometer in a quartz fluorescence cell. The fluorescence quantum yield was calculated using comparative method with quinine sulphate in 0.1 M H_2SO_4 as reference [52-54] as stated in Eq. (11).

$$\Phi_{f(s)} = \frac{\Phi_{f(r)} I_s A_r n_s^2}{I_r A_s n_r^2} \tag{11}$$

where Φ_f, I, A and n are the fluorescence quantum yield, area under the band, absorbance value at excitation wavelength and refractive index for sample (s) and reference (r) respectively.

The oscillator strength in solution, a measure of the *allowedness* and intensity of a transition, was calculated from the Eq. (12) [55].

$$f = \frac{2.303 m_e\, c^2 \varepsilon_o}{N_o e^2 n} \int \varepsilon_{\bar{\upsilon}} d\bar{\upsilon} \tag{12}$$

where m_e is the mass of electron, c is the speed of light in vacuum, e is the electronic charge, n is the refractive index of the solvent, ε_o is relative permittivity of free space, N_o is Avogadro's number, $\varepsilon_{\bar{\upsilon}}$ is the molar absorptivity of the solute at wavenumber, $\bar{\upsilon}$. The integral of the molar absorptivity with respect to the wavenumber was calculated as the area under each deconvoluted band. Eq. (12) could be simplified into

$$f = \frac{4.321 \times 10^{-9}}{n} \int \varepsilon_{\bar{\upsilon}} d\bar{\upsilon} \quad (13)$$

The oscillator strength at vapour phase, f_v, was calculated using Shuyer's expression for the classical extension of Lorentz field effect as adopted by Adeoye et al. [56].

$$\frac{f_s}{f_v} = \Phi \quad (14)$$

where f_s and f_v are the oscillator strengths in solution and vapour, respectively and Φ is the correction factor when the system changes from solution to vapour phase. Φ can be computed from the refractive index (n) of the solvent using Eq. (15):

$$\Phi = \frac{9n^3}{(2n^2+1)^2} \quad (15)$$

when $n = 0.361$ (for ethanol), $\Phi = 1.025$.

3.2. Synthesis of 2-(((5-aminonaphthalen-1-yl)imino)methyl)phenol (DANOHB)

0.79 g (0.005 mol) of 1,5-diaminonaphthalene was dissolved in 10 mL ethanol and added dropwise to hot and stirring ethanolic solution of 0.39 mL (0.005 mol) o-hydroxybenzaldehyde which afforded an immediate formation of yellow precipitate. The solution was further refluxed for 1 h to obtain the high yield product which was filtered and washed with cold ethanol and dichloromethane (Scheme 1). The residue was dried in the fume hood. Yield (1.19 g, 91%,); Melting point (214–216 °C); Molecular weight (M + 1) 263.09; Selected IR peaks (ATR, $\bar{\upsilon}$ cm^{-1}); 3391 ($NH_{2\ str}$), 1612 ($C{=}N_{str}$); ^1H NMR (300 MHz, $CDCl_3$) δ 13.33 (s, 1H), 8.72 (s, 1H), 8.21 (d, J = 8.5 Hz, 1H), 7.61–7.52 (m, 1H), 7.50–7.41 (m, 3H), 7.26 (t, J = 5.6 Hz, 2H), 7.11 (d, J = 8.2 Hz, 1H), 7.00 (t, J = 7.5 Hz, 1H), 6.78 (t, J = 4.2 Hz, 1H) ppm; ^{13}C NMR (75 MHz, $CDCl_3$) δ 164.00 (C=N), 161.30, 140.34, 142.72, 133.68, 132.63, 128.92, 126.67, 125.42, 124.53, 122.35, 119.58, 119.43, 117.44, 115.04, 111.68, 109.98 ppm; ^{13}C-DEPT 135 NMR (75 MHz, $CDCl_3$) δ 164.00 (azomethine H-C=N), 133.68, 132.63, 126.68, 125.42, 122.35, 119.43, 117.44, 115.04, 111.68, 109.98 ppm.

4. Results and discussion

4.1. Characterization of 2-(((5-aminonaphthalen-1-yl)imino)methyl)phenol (DANOHB)

The Schiff base, DANOHB, was characterized using 1-D (^1H, ^{13}C and ^{13}C-DEPT) NMR, 2-D (^1H—^1H COSY and HSQC) NMR, ATR-FTIR, mass spectrometry and melting point. The proton NMR spectrum of DANOHB shows a well resolved and symmetrical resonance of aromatic protons in the chemical shift range of δ 6.7 and 8.3 ppm. The azomethine peak is located downfield at a chemical shift of δ 8.72 ppm. The phenolic proton is sighted downfield in the spectrum as a sharp singlet peak at δ 13.33 ppm. ^{13}C proton decoupled NMR spectrum shows seventeen (17) peaks in the chemical shift range of δ 109–164 ppm. The C—H peak of the Schiff base is observed at δ 164.00 ppm which is further confirmed by ^{13}C-DEPT 135 spectrum. In addition to the azomethine peak, ten other peaks resonating as positive signals were observed in the DEPT 135 spectrum which could be assigned to C—H of the aromatic rings. From HSQC, the peak at δ 164.00 in the DEPT 135 spectrum is coupled to the proton at δ 8.72 ppm which was assigned to the azomethine hydrogen (See supplementary material).

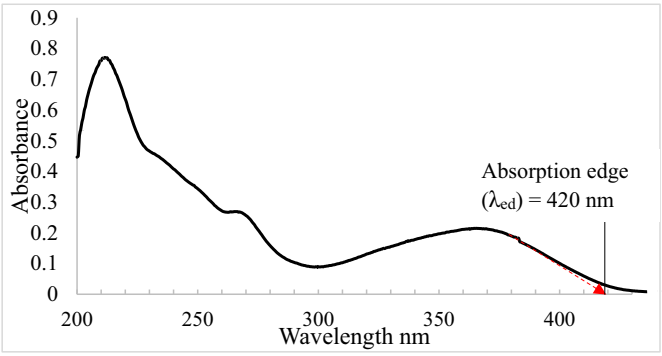

Fig. 1. Absorption spectrum of DANOHB in ethanol.

The infrared spectrum of the compound was run neat using attenuated total reflection technique. The O—H stretching vibration of the Schiff base occurs between 3400 and 2900 as a broad band which may be due to intramolecular and intermolecular hydrogen bond formation. The sharp peak at 1612 cm^{-1} could be assigned to imine C=N stretching vibrations. The vibrations between 1592 and 1400 cm^{-1} are assigned to aromatic C=C ring stretch. From the mass spectrum, the molecular ion $[M + 1]^+$ for the compound is obtained at 263.09 (See supplementary material). Also, the melting point is in the range of 214–216 °C.

4.2. Electronic spectra of DANOHB

4.2.1. Experimental absorption and emission spectra of DANOHB

Figs. 1 and 2 show the absorption spectra of DANOHB reported in wavelength and wavenumber, respectively. In Fig. 1, three absorption bands were observed for DANOHB in ethanol designated as Band I ($S_0 \rightarrow S_1$), Band II ($S_0 \rightarrow S_2$) and Band III ($S_0 \rightarrow S_3$) in order of increasing energy. The low-energy transition (Band I) appeared at 365 nm (absorption edge around 420 nm) as a moderately broad and smooth band with an oscillator strength of 0.05 and a low extinction coefficient. The low-energy absorption edge (λ_{ed}) at 420 nm, in line with calculated lowest energy transition, corresponds to a low band gap of 2.95 eV (that

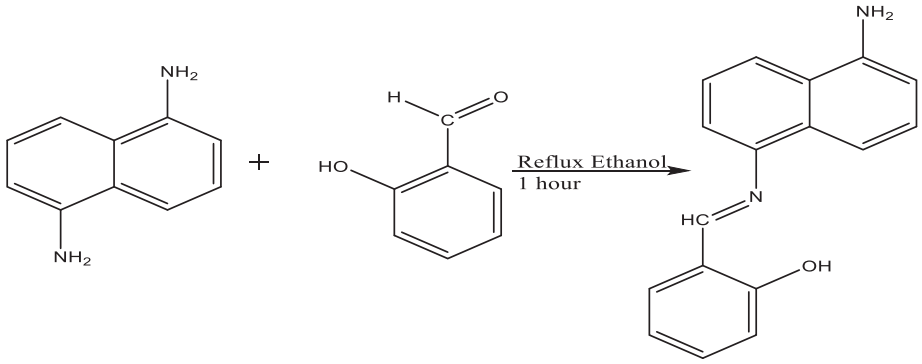

Scheme 1. Synthesis of DANOHB

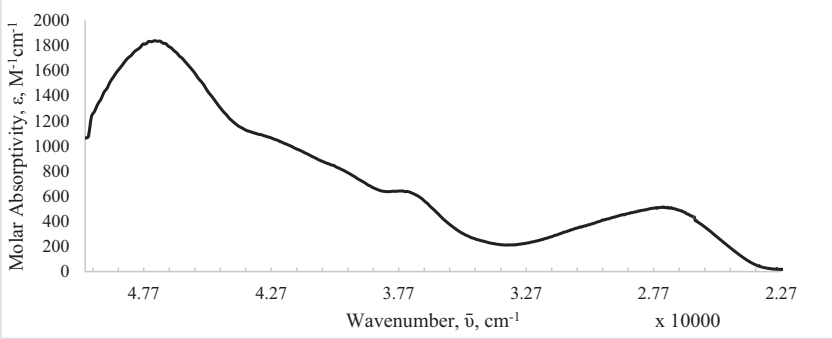

Fig. 2. Extinction coefficient against wavenumber for DANOHB in ethanol.

Table 1
Electronic absorption and emission properties of DANOHB in ethanol.

Compound (DANOHB)	λ/nm	$f_{(s)}$	$\bar{\upsilon}_{expt}/cm^{-1} \times 10^4$	$\varepsilon_{max}/M^{-1}\ cm^{-1} \times 10^4$	$f_{(v)}$	λ^{Em}_{max}/nm	0–0 transition (λ/ nm)	Stokes shift (Δλ)/nm	Φ_f
BAND I	365	0.05	2.8	4.8	0.05	404	384	39	0.21
BAND II	268	–	3.6	5.4	–				
BAND III	212	–	4.8	14.0	–				

f: oscillator strength; ῡ: wavenumber; ε: molar absorptivity; λ: wavelength; λ^{Em}_{max}/nm: emission peak; Φ_f: fluorescence quantum yield.
Note: subscripts *s* and *v* represent solution and vapour phase respectively.

is, $1240/\lambda_{ed}$ in eV) which is characteristic of materials applicable as organic semiconductors [57]. The low molar absorptivity and oscillator strength of the low-energy transition suggest that the band arises from a forbidden transition. Other bands appear at 268 and 212 nm (Table 1). The emission band of DANOHB taken in ethanol at excitation wavelength (λ_{Ex}) of 330 nm has its peak at 404 nm with a fluorescence quantum yield of 0.21. This indicates that the Stokes shift between the emission peak and absorption maximum (λ_{max}) for the low-energy transition is 39 nm (Fig. 3). Systems with large Stokes shift present reduced spectral overlap which minimizes the problem of photon reabsorption and have good applications in photovoltaic cells [34,58–60]. The wavelength of spectra overlap (0–0 transition) was obtained at 384 nm.

4.2.2. Calculated electronic absorption properties of DANOHB

Computed electronic absorption properties of DANOHB are reported in vacuum, cyclohexane and ethanol (Table 2). Eighteen excited states are calculated for the Schiff base from which two high intensity bands arise (Fig. 4). The lowest energy transition appeared at 433.38 nm (2.86 eV) in ethanol with an oscillator strength (*f*) of 0.24 and was predicted to arise from HOMO-LUMO transition which corresponds to the experimental low-energy absorption band. The low oscillator strength, depicting the forbidden nature of this transition, is in line with the experimental value. Negative solvatochromism, exhibited by the lowest energy transition as the solvent polarity increases, suggests that the ground state is more polar than the excited which results into the stabilization of the ground state relative to the excited state [61]. The

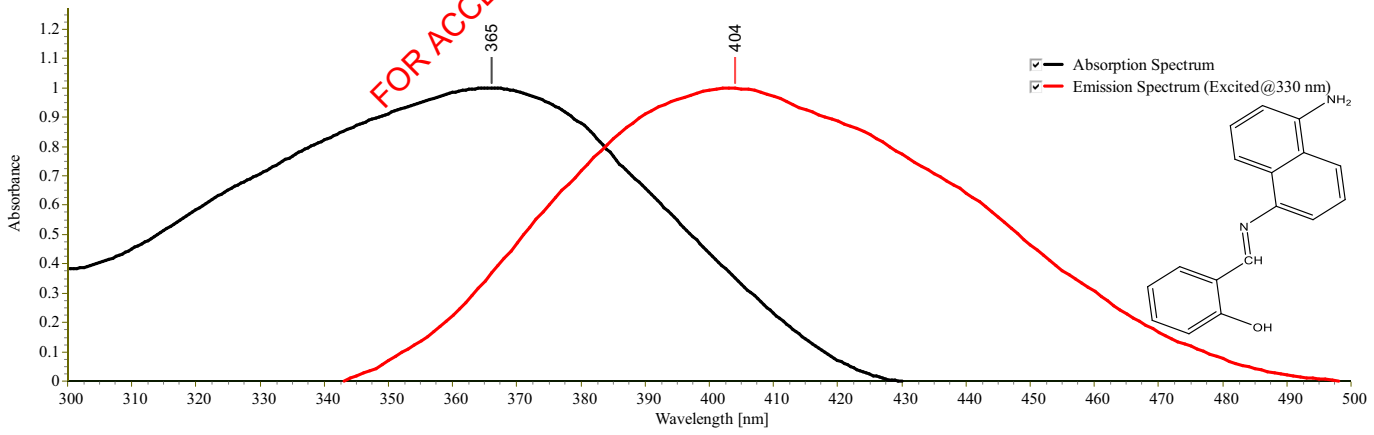

Fig. 3. Normalized absorption (black) and emission (red) spectra of DANOHB in ethanol ($\lambda_{Ex} = 330$ nm).

Table 2
TD-DFT/B3LYP/6-311++G(d,p) result of excited states, orbitals, excitation energies (EE), wavelength (λ) and oscillator strength (*f*) of DANOHB in vacuum, cyclohexane and ethanol.

Excited states	Orbitals	Vacuum			Cyclohexane			Ethanol		
		EE	λ/nm	*f*	EE	λ/nm	*f*	EE	λ/nm	*f*
1	H-L	2.81	441.36	0.17	2.82	440.43	0.24	2.86	433.38	0.24
2	H-L + 1	3.93	315.83	0.20	3.90	318.20	0.28	3.89	318.65	0.24

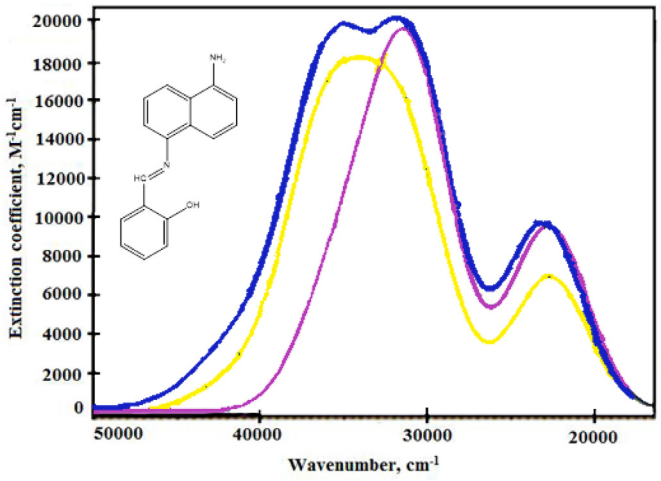

Fig. 4. Stacked UV-visible absorption spectra of DANOHB in vacuum (yellow), cyclohexane (purple) and ethanol (blue) using TD-DFT/B3LYP/6-311++G(d,p).

observed sensitivity of the low-energy band to medium polarity implies that the reactivity of the Schiff base would be enhanced in less polar medium. Another high intensity transition observed at 315.83 nm (3.90 eV), with notable bathochromic and hyperchromic shifts as solvent polarity increases, indicates a more polar excited state than the ground state leading to a relative stabilization of the excited state. Bands II and III in vacuum and cyclohexane exhibit a notable overlap which is slightly resolved in ethanol.

4.3. Quantum chemical calculations

4.3.1. Quantum chemical descriptors of stability and chemical reactivity

Fig. 5 shows the optimized structure of DANOHB. Table 3 shows the result of the quantum chemical calculations carried out on DANOHB in vacuum, cyclohexane and ethanol. The total energy of the system, energy of the lowest unoccupied molecular orbital (E_{LUMO}), energy of the highest occupied molecular orbital (E_{HOMO}) and the energy gap (ΔE) were calculated and reported. The thermodynamic stability of DANOHB is related to the total energy of the system (E = −841.19 a.u.). This parameter was observed to decrease as the polarity of the medium increased which implies that better thermodynamic stability is conferred on the system in polar environment.

Moreover, the reactivity of the compound is a function of the energies of the frontier orbitals. E_{HOMO} is related to the electron donating ability of a molecule. According to Koopman's theorem, this parameter

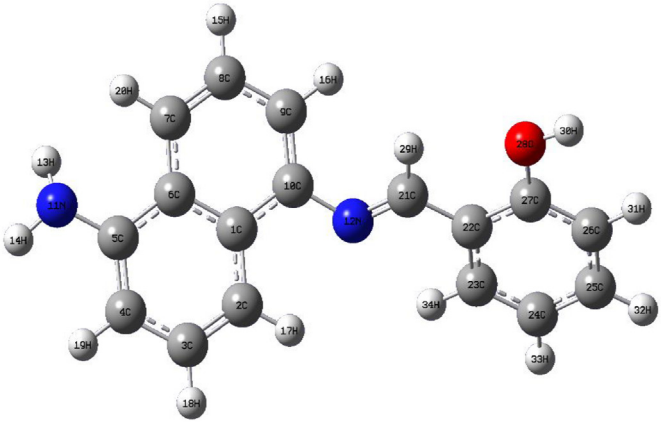

Fig. 5. B3LYP optimized structure of DANOHB.

Table 3
Quantum chemical parameters of DANOHB.

Compound	Energy (au)	E_{LUMO} (eV)	E_{HOMO} (eV)	ΔE (eV)
DANOHB in vacuum	−841.19	−1.93	−5.24	3.31
DANOHB in cyclohexane	−841.20	−1.98	−5.33	3.35
DANOHB in ethanol	−841.21	−2.11	−5.51	3.40

is used to calculate the ionization potential (I) of a system [62–64]. E_{HOMO} value for the Schiff base was observed to decrease with increase in solvent polarity. E_{LUMO}, a parameter which is related to the electron affinity (A) of a system, follows the same trend with E_{HOMO} as it increases with increase in the polarity of the medium. In addition, E_{LUMO} of this Schiff base is best stabilized in ethanol (−2.11 eV) which suggests a low-lying conduction band and good electron affinity of the system in the polar environment. The energy gap ($\Delta E = E_{LUMO} - E_{HOMO}$) is a descriptor of the reactivity of a molecule which increases as its energy gap decreases. The low energy gap of the Schiff base indicates the potential of the compound as an organic semiconductor. This parameter is observed to be destabilized as the polarity of the solvent increases which could be attributed to better stabilization of the HOMO relative to LUMO. This destabilization of band gap suggests a better semiconducting potential of the Schiff base in less polar medium.

4.3.2. Quantum chemical descriptors of molecular polarity and nonlinear optical activities

Table 4 shows the dipole moment of DANOHB in the chosen media of varied dielectric constant. The highest contribution to the dipole moment arises from the x-component and the magnitude increases with solvent polarity. In the same vein, the total static dipole moment (μ) in the gas solvent is 1.94 D which increases as the medium polarity increases. This may be attributed to better charge separation in polar medium.

From the quadrupolar components, the mean polarizability was calculated and reported in Table 5. The quadrupole moment along the α_{zz} coordinate gives a major contribution to the polarizability tensor of the imine system. Since the mean polarizability of the Schiff base decreases with increasing solvent polarity, it could be inferred that less distortion of electron cloud is operative in polar environment and a decrease in molecular size. Anisotropy of polarizability also obtained is solvent dependent and increases in polar media. This implies that the applicability of the Schiff base in nonlinear optical applications like optical telecommunications would be preferred in less polar environment [65].

Diagonal and off-diagonal octupolar components of first hyperpolarizability in vacuum, cyclohexane and ethanol of DANOHB are reported in Table 6. Except for the β_{xyy} component, other components show an increase in magnitude with increase in solvent polarity

Table 4
Dipole moment (μ) and its components for DANOHB in vacuum, cyclohexane and ethanol.

Compound	μ_x	μ_y	μ_z	μ/Debye
DANOHB in vacuum	1.77	0.80	0.08	1.94
DANOHB in cyclohexane	1.99	0.98	0.16	2.22
DANOHB in ethanol	2.25	1.40	0.25	2.66

Table 5
Mean polarizability, components of polarizability and polarizability anisotropy of DANOHB.

Compound	α_{xx}	α_{yy}	α_{zz}	<α>/a.u.	Δα/a.u.
DANOHB in vacuum	77.22	108.31	121.79	102.44	43.58
DANOHB in cyclohexane	72.48	107.72	121.65	100.61	48.21
DANOHB in ethanol	63.42	106.25	121.68	97.12	56.94

Table 6
Octupolar components of DANOHB in vacuum, cyclohexane and ethanol.

Compound	β_{xxx}	β_{xyy}	β_{xzz}	β_{xxy}	β_{yyy}	β_{yzz}	β_{xxz}	β_{yyz}	β_{zzz}
DANOHB in vacuum	21.24	3.99	25.44	7.73	11.01	5.97	10.04	0.23	10.31
DANOHB in cyclohexane	25.22	3.29	27.58	8.18	11.97	6.37	10.88	0.32	10.98
DANOHB in ethanol	29.63	2.04	30.20	10.24	14.29	7.10	12.49	0.32	11.57

as the largest contributions to the third rank tensor are along the xxx and xzz coordinates. The dipolar components of hyperpolarizability and the total hyperpolarizability (β_{tot}) in the selected media are reported in Table 7. Note-worthy, however, is the higher value calculated for the total first-order hyperpolarizability (β_{tot}) of this Schiff base than the urea (standard NLO material) at the same level of theory. β_{tot} for DANOHB is observed to be about three times higher than that of urea. Hence, the Schiff base exhibits second harmonic generation potentials which is enhanced by increase in solvent polarity.

The microscopic descriptor of the third harmonic generation (THG) computed in terms of the second order hyperpolarizability (γ) and its hexadecapole moment are reported in Table 8. Absolute value of γ is reported in S.I. unit and observed to decrease with increase in solvent polarity. This third-order nonlinear optical parameter is more than thirty (30) times larger than that of urea. Major contribution to the second-order hyperpolarizability arises from γ_{xxxx} and the amplitude is observed to be solvent-dependent. Materials with better hyperpolarizabilities than urea are applicable in optical switching, optical modulation, optical data storage devices and fiber-optic telecommunication.

5. Conclusions

Synthesis of 2-(((5-aminonaphthalen-1-yl)imino)methyl)phenol (DANOHB) has been achieved from one-step condensation and characterization achieved using spectroscopic techniques. Solvent plays a major role in enhancing or damping the electronic and nonlinear optical properties of the Schiff base. The experimental low-energy absorption edge is in agreement with the calculated lowest energy transition which suggests a low band gap and, consequently, good potential as an organic semiconductor. The compound exhibits fluorescence with a fairly large Stokes shift which implies a reduced photon reabsorption and better effectiveness for photoluminescent applications. From density functional calculations, the nonlinear optical properties of the Schiff base are better than that of urea standard which indicates that the material has good potentials for nonlinear optical applications. In polar environment, the first hyperpolarizability (second harmonic generation property) of the Schiff base is enhanced while the second hyperpolarizability is slightly damped.

Table 7
Dipolar first hyperpolarizability components and total hyperpolarizability of DANOHB.

Compound	β_x/a.u.	β_y/a.u.	β_z/a.u.	β_{tot}/a.u.	$\beta_{tot}/10^{-53}$ $C^3m^3J^{-2}$
DANOHB in vacuum	50.67	24.70	20.58	60.01	192.42
DANOHB in cyclohexane	56.09	26.52	22.18	65.89	211.26
DANOHB in ethanol	64.49	28.69	22.60	74.11	237.63

Urea: $\beta_{tot} = 57.68 \times 10^{-53}$ $C^3m^3J^{-2}$.

CRediT authorship contribution statement

Nathanael Damilare Ojo: Conceptualization, Data curation, Formal analysis, Funding acquisition, Investigation, Methodology, Project administration, Resources, Writing - original draft, Writing - review & editing. **Rui Werner Krause:** Resources, Supervision, Conceptualization, Validation, Methodology. **Nelson Okpako Obi-Egbedi:** Resources, Supervision, Conceptualization, Methodology, Validation, Visualization, Software, Formal analysis, Writing - review & editing.

Declaration of competing interest

The authors declare that they have no known competing financial interests or personal relationships that could have appeared to influence the work reported in this paper.

Acknowledgements

The research was supported by Tertiary Education Trust Fund (TETFUND). The effort of Dr. Xavier Siwe Noundou who assisted in running and processing the high-resolution mass spectrum of this compound is greatly appreciated.

Appendix A. Supplementary data

Supplementary data to this article can be found online at https://doi.org/10.1016/j.molliq.2020.114157.

References

[1] W.P. Silva, E. Girotto, H. Gallardo, R. Cristiano, Synthesis and characterization of photoactive columnar liquid crystals containing azobenzene and quinoxaline moieties, J. Mol. Liq. 307 (2020) 1–11, https://doi.org/10.1016/j.molliq.2020.112944.
[2] V. Manzoni, L. Modesto-Costa, J. Del Nero, T. Andrade-Filho, R. Gester, Strong enhancement of NLO response of methyl orange dyes through solvent effects: a sequential Monte Carlo/DFT investigation, Opt. Mater. (Amst). 94 (2019) 152–159, https://doi.org/10.1016/j.optmat.2019.05.018.
[3] M.F. Khan, R. Bin Rashid, M.Y. Mian, M.S. Rahman, M.A. Rashid, Effects of solvent polarity on solvation free energy, dipole moment, polarizability, hyperpolarizability and molecular properties of metronidazole, Bangladesh Pharm. J. 19 (2016) 9–14, https://doi.org/10.3329/bpj.v19i1.29229.
[4] T.T. Tidwell, Hugo (Ugo) Schiff, Schiff bases, and a century of β-lactam synthesis, Angew. Chem. Int. Ed. 47 (2008) 1016–1020, https://doi.org/10.1002/anie.200702965.
[5] A.S.A. Dena, To the memory of Hugo Schiff: applications of Schiff bases in potentiometric sensors, Russ. J. Appl. Chem. 87 (2014) 383–396, https://doi.org/10.1134/S1070427214030227.
[6] B. Prathima, Y. Subba Rao, S. Adinarayana Reddy, Y.P. Reddy, A. Varada Reddy, Copper(II) and nickel(II) complexes of benzyloxybenzaldehyde-4-phenyl-3-thiosemicarbazone: synthesis, characterization and biological activity, Spectrochim. Acta - Part A Mol. Biomol. Spectrosc. 77 (2010) 248–252, https://doi.org/10.1016/j.saa.2010.05.016.
[7] T. Arun, S. Packianathan, M. Malarvizhi, R. Antony, N. Raman, Bio-Relevant Complexes of Novel N_2O_2 Type Heterocyclic Ligand: Synthesis, Structural Elucidation, Biological Evaluation and Docking Studies, Elsevier B.V, 2015https://doi.org/10.1016/j.jphotobiol.2015.05.022.
[8] N. Turan, E. Kaya, B. Gündüz, N. Çolak, H. Körkoca, Synthesis, characterization of poly (E)-3-amino-4-((3-bromophenyl)diazenyl)-1H-pyrazol-5-ol: investigation of antibacterial activity, fluorescence, and optical properties, Fibers Polym. 13 (2012) 415–424, https://doi.org/10.1007/s12221-012-0415-2.

Table 8
Second order hyperpolarizability (γ) and its hexadecapole moments.

Compound	γ_{xxxx}/ a.u.	γ_{yyyy}/ a.u.	γ_{zzzz}/ a.u.	γ_{xxyy}/ a.u.	γ_{xxzzz}/ a.u.	γ_{yyzz}/ a.u.	$\gamma/10^{-65}$ ($C^4m^4J^{-3}$)
DANOHB in vacuum	−6817.25	−1397.17	−393.19	−1521.53	−1558.69	−306.24	19,180.67
DANOHB in cyclohexane	−6616.54	−1380.13	−399.18	−1507.44	−1552.24	−303.74	18,859.15
DANOHB in ethanol	−6236.57	−1353.11	−404.36	−1476.30	−1545.65	−300.32	18,255.43

Urea: $\gamma = 591 \times 10^{-65}$ $C^4m^4J^{-3}$.

[9] I. Ismiyarto, N. Rizki, N. Ngadiwiyana, P.R. Sarjono, N.B.A. Prasetya, Synthesis of derivatives azomethine compounds bonded to alkoxylated benzene and their antibacterial activity tests, J. Phys. Conf. Ser. 1524 (2020) 1–9, https://doi.org/10.1088/1742-6596/1524/1/012090.

[10] M. Grigoras, N.C. Antonoaia, Synthesis and characterization of some carbazole-based imine polymers, Eur. Polym. J. 41 (2005) 1079–1089, https://doi.org/10.1016/j.eurpolymj.2004.11.019.

[11] S. Tarkuc, E.K. Unver, Y.A. Udum, L. Toppare, Multi-colored electrochromic polymer with enhanced optical contrast, Eur. Polym. J. 46 (2010) 2199–2205, https://doi.org/10.1016/j.eurpolymj.2010.08.002.

[12] E. Schab-Balcerzak, M. Grucela-Zajac, M. Krompiec, A. Niestroj, H. Janeczek, New low band gap compounds comprised of naphthalene diimide and imine units, Synth. Met. 162 (2012) 543–553, https://doi.org/10.1016/j.synthmet.2012.01.016.

[13] R. Kumari, S.K. Sahu, Effect of solvent-derived highly luminescent multicolor carbon dots for white-light-emitting diodes and water detection, Langmuir 36 (2020) 5287–5295, https://doi.org/10.1021/acs.langmuir.0c00631.

[14] A. Singh, U. Nishith, D.R. Trivedi, Spectroscopic studies of colorimetric receptors for detection of biologically important inorganic F^-, AcO^- and $H_2PO_4^-$ anions in organo-aqueous medium: real-life application, Inorg. Chem. Commun. 115 (2020) 1–11, https://doi.org/10.1016/j.inoche.2020.107874.

[15] S.I. Hazarika, A.K. Atta, Carbohydrate-based fluorometric and colorimetric sensors for Cu^{2+} ion recognition, Comptes Rendus Chim. 22 (2019) 599–613, https://doi.org/10.1016/j.crci.2019.07.003.

[16] A.A. Abdulridha, M.A. Albo Hay Allah, S.Q. Makki, Y. Sert, H.E. Salman, A.A. Balakit, Corrosion inhibition of carbon steel in 1 M H_2SO_4 using new Azo Schiff compound: electrochemical, gravimetric, adsorption, surface and DFT studies, J. Mol. Liq. 315 (2020), 113690https://doi.org/10.1016/j.molliq.2020.113690.

[17] B. Andr, J. Pedras, Synthesis, Characterization and Applications of New Schiff Base Fluorescent Chemosensors for Metal and DNA Interactions: Conventional and "Green" Approaches, 2011 1–227https://run.unl.pt/bitstream/10362/9684/1/Pedras_2011.pdf.

[18] I. Pietro Oliveri, Zinc(II) Schiff base complexes and their aggregation/deaggregation properties: versatile and multifunctional materials as chemosensors and building blocks for new supramolecular architectures, (2012) 1–222. http://dspace.unict.it/bitstream/10761/1292/1/LVRVPT86D01C351S-PhD%20thesis.pdf.

[19] A. Prakash, D. Adhikari, Application of Schiff bases and their metal complexes-a review, Int. J. ChemTech Res. 3 (2011) 1891–1896http://sphinxsai.com/Vol.3No.4/chem/pdf/CT=26(1891-1896)OD11.pdf.

[20] S. Leela, R. Hema, H. Stoeckli-evans, K. Ramamurthi, G. Bhagavannarayana, Design, synthesis, growth and characterization of 4-methoxy-4-dimethylaminobenzylidene aniline (MDMABA): a novel third order nonlinear optical material, Spectrochim. Acta Part A Mol. Biomol. Spectrosc. 77 (2010) 927–932, https://doi.org/10.1016/j.saa.2010.08.012.

[21] S. Shokrollahi, A. Amiri, F.F. Tirani, K. Schenk-Joß, Promising anti-cancer potency of 4,5,6,7-tetrahydrobenzo[d]thiazole-based Schiff-bases, J. Mol. Liq. (2018)https://doi.org/10.1016/j.molliq.2019.112262.

[22] G. Ceyhan, M. Köse, M. Tümer, I. Demirtaş, A. Şahin Yağlioğlu, V. McKee, Structural characterization of some Schiff base compounds: investigation of their electrochemical, photoluminescence, thermal and anticancer activity properties, J. Lumin. 143 (2013) 623–634, https://doi.org/10.1016/j.jlumin.2013.06.002.

[23] A.M. Asiri, S.A. Khan, H.M. Marwani, K. Sharma, Synthesis, spectroscopic and physicochemical investigations of environmentally benign heterocyclic Schiff base derivatives as antibacterial agents on the bases of in vitro and density functional theory, J. Photochem. Photobiol. B 120 (2013) 82–89, https://doi.org/10.1016/j.jphotobiol.2013.01.007.

[24] S. Harpstrite, S. Collins, A. Oksman, D. Goldberg, V. Sharma, Synthesis, characterization, and antimalarial activity of novel Schiff-base-phenol and naphthalene-amine ligands, Med. Chem. (Los Angeles) 4 (2008) 392–395, https://doi.org/10.2174/157340608784872280.

[25] M.A. Ashraf, K. Mahmood, A. Wajid, M.J. Maah, I. Yusoff, Synthesis, characterization and biological activity of Schiff bases, Int. Conf. Chem. Chem. Proc. 10 (2011) 1–7http://citeseerx.ist.psu.edu/viewdoc/download?doi=10.1.1.1013.13&rep=rep1&type=pdf.

[26] Y. Tao, K. Yuan, T. Chen, P. Xu, H. Li, R. Chen, C. Zheng, Thermally Activated Delayed Fluorescence Materials Towards the Breakthrough of Organoelectronics, 2014 1–28, https://doi.org/10.1002/adma.201402532.

[27] D. Zhang, X. Zhang, Crystallization and Characterization of a New Fluorescent Molecule Based on Schiff Base, vol. 2013, 2013 28–30, https://doi.org/10.4236/jcpt.2013.31004.

[28] M. Hosseini, Z. Vaezi, M.R. Ganjali, F. Faridbod, S.D. Abkenar, K. Alizadeh, M. Salavati-Niasari, Fluorescence "turn-on" chemosensor for the selective detection of zinc ion based on Schiff-base derivative, Spectrochim. Acta - Part A Mol. Biomol. Spectrosc. 75 (2010) 978–982, https://doi.org/10.1016/j.saa.2009.12.016.

[29] T.B. Wei, G.Y. Gao, W.J. Qu, B.B. Shi, Q. Lin, H. Yao, Y.M. Zhang, Selective fluorescent sensor for mercury(II) ion based on an easy to prepare double naphthalene Schiff base, Sensors Actuators B Chem. 199 (2014) 142–147, https://doi.org/10.1016/j.snb.2014.03.084.

[30] M. Köse, G. Ceyhan, M. Tümer, I. Demirtaş, İ. Gönül, V. McKee, Monodentate Schiff base ligands: their structural characterization, photoluminescence, anticancer, electrochemical and sensor properties, Spectrochim. Acta A Mol. Biomol. Spectrosc. 137 (2015) 477–485, https://doi.org/10.1016/j.saa.2014.08.088.

[31] P.S. Perlepe, L. Cunha-Silva, K.J. Gagnon, S.J. Teat, C. Lampropoulos, A. Escuer, T.C. Stamatatos, "Ligands-with-benefits": naphthalene-substituted Schiff bases yielding new Ni II metal clusters with ferromagnetic and emissive properties and undergoing exciting transformations, Inorg. Chem. 55 (2016) 1270–1277, https://doi.org/10.1021/acs.inorgchem.5b02492.

[32] S. Arulmurugan, H.P. Kavitha, B.R. Venkatraman, Biological activities of Schiff base and its complexes : a review, Rasayan J. Chem. 3 (2010) 385–410https://rasayanjournal.co.in/vol-3/issue-3/1.pdf.

[33] T. Kumpulainen, B. Lang, A. Rosspeintner, E. Vauthey, Ultrafast elementary photochemical processes of organic molecules in liquid solution, Chem. Rev. 117 (2017) 10826–10939, https://doi.org/10.1021/acs.chemrev.6b00491.

[34] V.M. Granchak, T.V. Sakhno, S.Y. Kuchmy, Light-emitting materials – active components of luminescent solar concentrators, Theor. Exp. Chem. 50 (2014) 1–20, https://doi.org/10.1007/s11237-014-9342-1.

[35] N. Nwaji, B. Jones, J. Mack, D.O. Oluwole, T. Nyokong, Nonlinear optical dynamics of benzothiazole derivatized phthalocyanines in solution, thin films and when conjugated to nanoparticles, J. Photochem. Photobiol. A Chem. 346 (2017) 46–59, https://doi.org/10.1016/j.jphotochem.2017.05.042.

[36] M. de Wergifosse, S. Grimme, Nonlinear-response properties in a simplified time-dependent density functional theory (sTD-DFT) framework: evaluation of the first hyperpolarizability, J. Chem. Phys. 149 (2018), 024108https://doi.org/10.1063/1.5037665.

[37] M. Kurban, B. Gündüz, Physical and optical properties of DCJTB dye for OLED display applications: experimental and theoretical investigation, J. Mol. Struct. 1137 (2017) 403–411, https://doi.org/10.1016/j.molstruc.2017.02.064.

[38] C. Fang, B. Durbeej, Calculation of free-energy barriers with TD-DFT: a case study on excited-state proton transfer in indigo, J. Phys. Chem. A 123 (2019) 8485–8495, https://doi.org/10.1021/acs.jpca.9b05163.

[39] É.A.G. Brémond, J. Kieffer, C. Adamo, A reliable method for fitting TD-DFT transitions to experimental UV-visible spectra, J. Mol. Struct. THEOCHEM 954 (2010) 52–56, https://doi.org/10.1016/j.theochem.2010.04.038.

[40] A. Sharma, A. Barakat, H.H. Al-Rasheed, A.M. Al-Majid, S. Yousuf, M.I. Choudhary, A. El-Faham, B.G. de la Torre, F. Albericio, Crystal structure and theoretical investigation of thiobarbituric acid derivatives as nonlinear optical (NLO) materials, Crystals 10 (2020) 1–14, https://doi.org/10.3390/cryst10060442.

[41] G. Berger, Synthesis of chiral vicinal diamines and in vitro anticancer properties of their platinum(II) coordinates, https://pdfs.semanticscholar.org/f049/f6466beadc7f46a6542fdf952e3db3c0872d.pdf 2013.

[42] E. Papajak, J. Zheng, X. Xu, H.R. Leverentz, D.G. Truhlar, Perspectives on basis sets beautiful: seasonal plantings of diffuse basis functions, J. Chem. Theory Comput. 7 (2011) 3027–3034, https://doi.org/10.1021/ct200106a.

[43] P.M. Warner, Ab initio calculations on heteroatomic systems using density functional theory and diffuse basis functions, J. Organomet. Chem. 61 (1996) 7192–7194, https://doi.org/10.1021/jo952259j.

[44] G. Maroulis, T. Bancewicz, B. Champagne, A.D. Buckingham, Atomic and Molecular Nonlinear Optics: Theory, Experiment and Computation: A Homage to the Pioneering Work of Stanislaw Kielich (1925–1993), 2011.

[45] H. Soscún, Ab initio and DFT study of the static dipole (hyper)polarizabilities of benzaldehyde and thio-benzaldehyde molecules in gas phase, J. Comput. Methods Sci. Eng. 10 (2010) 573–583, https://doi.org/10.3233/JCM-2010-0345.

[46] S. Sudha, M. Karabacak, M. Kurt, M. Cinar, N. Sundaraganesan, Molecular structure, vibrational spectroscopic, first-order hyperpolarizability and HOMO, LUMO studies of 2-aminobenzimidazole, Spectrochim. Acta - Part A Mol. Biomol. Spectrosc. 84 (2011) 184–195, https://doi.org/10.1016/j.saa.2011.09.028.

[47] F.A. Khazaal, M.M. Kadhim, H.F. Husseein, Z.M. Abbas, M.S. Hamzah, I.A. Khudhair, H.A. Almashhadani, H.H. Abed, H.S. Saieed, Electronic transfers and (NLO) properties predicted by ab initio methods with prove experimentally, NeuroQuantology 18 (2020) 46–51, https://doi.org/10.14704/nq.2020.18.1.NQ20106.

[48] M.J. Frisch, G.W. Trucks, H.B. Schlegel, G.E. Scuseria, M.A. Robb, J.R. Cheeseman, G. Scalmani, V. Barone, B. Mennucci, G.A. Petersson, H. Nakatsuji, M. Caricato, X. Li, H.P. Hratchian, A.F. Izmaylov, J. Bloino, G. Zheng, J.L. Sonnenberg, M. Hada, M. Ehara, K. Toyota, R. Fukuda, J. Hasegawa, M. Ishida, T. Nakajima, Y. Honda, O. Kitao, H. Nakai, T. Vreven, J.A. Montgomery Jr., J.E. Peralta, F. Ogliaro, M. Bearpark, J.J. Heyd, E. Brothers, K.N. Kudin, V.N. Staroverov, R. Kobayashi, J. Normand, K. Raghavachari, A. Rendell, J.C. Burant, S.S. Iyengar, J. Tomasi, M. Cossi, N. Rega, J.M. Millam, M. Klene, J.E. Knox, J.B. Cross, V. Bakken, C. Adamo, J. Jaramillo, R. Gomperts, R.E. Stratmann, O. Yazyev, A.J. Austin, R. Cammi, C. Pomelli, J.W. Ochterski, R.L. Martin, K. Morokuma, V.G. Zakrzewski, G.A. Voth, P. Salvador, J.J. Dannenberg, S. Dapprich, A.D. Daniels, O. Farkas, J.B. Foresman, J.V. Ortiz, J. Cioslowski, D.J. Fox, Gaussian, Inc., Wallingford CT, (2009).

[49] H. Tanak, Crystal structure, spectroscopy, and quantum chemical studies of (E)-2-[(2-chlorophenyl)iminomethyl]-4-trifluoromethoxyphenol, J. Phys. Chem. A 115 (2011) 13865–13876, https://doi.org/10.1021/jp205788b.

[50] P. Madhu, A.P. Munusamy, Effects of the bridge unit in D-π-A architecture to improve light harvesting efficiency at DSSCs: a first principle theoretical study, Environ. Prog. Sustain. Energy 37 (2018) 1403–1410, https://doi.org/10.1002/ep.12787.

[51] M.F. Khan, R. Bin Rashid, A. Hossain, M.A. Rashid, Computational study of solvation free energy, dipole moment, polarizability, hyperpolarizability and molecular properties of betulin, a constituent of Corypha taliera (Roxb.), Dhaka Univ. J. Pharm. Sci. 16 (2017) 1–8, https://doi.org/10.3329/dujps.v16i1.33376.

[52] N. Nwaji, D.O. Oluwole, J. Mack, M. Louzada, S. Khene, J. Britton, T. Nyokong, Improved nonlinear optical behaviour of ball type indium(III) phthalocyanine linked to glutathione capped nanoparticles, Dyes Pigments 140 (2017) 417–430, https://doi.org/10.1016/j.dyepig.2017.01.066.

[53] T.S. Singh, P.C. Paul, H.A.R. Pramanik, Fluorescent chemosensor based on sensitive Schiff base for selective detection of Zn^{2+}, Spectrochim. Acta A Mol. Biomol. Spectrosc. 121 (2014) 520–526, https://doi.org/10.1016/j.saa.2013.11.002.

[54] A. Fashina, E. Amuhaya, T. Nyokong, Photophysical studies of newly derivatized mono substituted phthalocyanines grafted onto silica nanoparticles via click chemistry, Spectrochim. Acta - Part A Mol. Biomol. Spectrosc. 140 (2015) 256–264, https://doi.org/10.1016/j.saa.2014.12.070.

[55] S.A. Ahmed, N.O. Obi-Egbedi, N.W. Odozi, I. Iweibo, M.D. Adeoye, Effects of solvent on the UV-visible absorption spectra of acenaphtho(1,2-b)quinoxaline and acenaphtho(1,2-b)benzo(g)quinoxaline, Afr. J. Pure Appl. Chem. 5 (2011) 393–397http://www.academicjournals.org/AJPAC.
[56] M.D. Adeoye, N.O. Obi-Egbedi, I. Iweibo, Solvent effect and photo-physical properties of 2,3-diphenylcyclopropenone, Arab. J. Chem. 10 (2017) S134–S140, https://doi.org/10.1016/j.arabjc.2012.06.019.
[57] Y. Li, Z. Wang, X. Cai, K. Liu, J. Dong, S. Chang, S.J. Su, Spiro[fluorene-9,9′-thioxanthene] core based host materials for thermally activated delayed fluorescence devices, Dyes Pigments 163 (2019) 249–256, https://doi.org/10.1016/j.dyepig.2018.12.001.
[58] Q. Wei, Y. Zhao, Q. Di, J. Liu, M. Xu, J. Liu, J. Zhang, Good dispersion of large-stokes-shift heterovalent-doped CdX quantum dots into bulk PMMA matrix and their optical properties characterization, J. Phys. Chem. C 121 (2017) 6152–6159, https://doi.org/10.1021/acs.jpcc.7b00207.
[59] C. Yang, J. Zhang, W.T. Peng, W. Sheng, D. Liu, P.S. Kuttipillai, M. Young, M.R. Donahue, B.G. Levine, B. Borhan, R.R. Lunt, Impact of stokes shift on the performance of near-infrared harvesting transparent luminescent solar concentrators, Sci. Rep. 8 (2018) 1–10, https://doi.org/10.1038/s41598-018-34442-3.
[60] G. Volpi, G. Magnano, I. Benesperi, D. Saccone, E. Priola, V. Gianotti, M. Milanesio, E. Conterosito, C. Barolo, G. Viscardi, One pot synthesis of low cost emitters with large Stokes' shift, Dyes Pigments 137 (2017) 152–164, https://doi.org/10.1016/j.dyepig.2016.09.056.
[61] A.A. Akande, N.O. Obi-Egbedi, N.D. Ojo, Effects of solvents on the electronic and molecular properties of 4-((2-methyl-4-nitrophenyl)iminomethyl)phenol, Int. J. Adv. Sci. Res. Eng. 5 (2019) 102–108, https://doi.org/10.31695/ijasre.2019.33455.
[62] N.O. Obi-egbedi, I.B. Obot, Inhibitive properties, thermodynamic and quantum chemical studies of alloxazine on mild steel corrosion in H_2SO_4, Corros. Sci. 53 (2011) 263–275, https://doi.org/10.1016/j.corsci.2010.09.020.
[63] I.B. Obot, N.O. Obi-Egbedi, HSAB descriptors of thiadiazole derivatives calculated by DFT: possible relationship as mild steel corrosion inhibitors, Der. Pharma. Chem. 1 (2009) 106–123.
[64] R. Chadli, M. Elazouzi, I. Khelladi, A.M. Elhourri, H. Elmsellem, Electrochemical and theoretical study of pyrazole 4-(4,5-dihydro-1H-pyrazol-5-yl)-N,N-dimethylaniline (D) as a corrosion inhibitor for mild steel in 1 M HCl, Port. Electrochim. Acta 35 (2017) 65–80, https://doi.org/10.4152/pea.201702065.
[65] S. Di Bella, I. Fragalà, I. Ledoux, J. Zyss, Dipolar donor-acceptor-substituted schiff base complexes with large off-diagonal second-order nonlinear optical tensor components, Chemistry 7 (2001) 3738–3743, https://doi.org/10.1002/1521-3765(20010903)7:17<3738::AID-CHEM3738>3.0.CO;2-I.